Expression, purification, and characterization of the M3M4 intracellular region of the human Zn^{2+} transporter protein, ZIP4

A Major Qualifying Project Report

Submitted to the Faculty of the

WORCESTER POLYTECHNIC INSTITUTE

In partial fulfillment of the requirements for the

Degree of Bachelor of Science

In Biochemistry/Biology & Biotechnology

by

Benjamin Morehouse

_____

&

Emily Rozsahegyi

_____

Date: April 2012

Approved:

Prof. Robert Dempski, Major Advisor

_____

Prof. Arne Gericke, Head of Chemistry and Biochemistry Department

_____

ABSTRACT

The goal of this project was to express, purify, and characterize the M3M4 intracellular region of the ZIP4 protein. This region has a series of histidine residues, which have a high zinc binding affinity. The zinc binding affinity and induced conformational change of the M3M4 region was measured using isothermal titration calorimetry and circular dichroism. The result of this project was the standardization and optimization of the protein purification protocol and zinc binding assays, as well as confirmation of previous data.

ACKNOWLEDGEMENTS

Firstly, we would like to thank our project advisor and lab head Robert Dempski Ph.D. for the invitation to work on this project and for his support and guidance along the way.

We also thank Sagar Antala for showing up when he didn't need to, staying late when he didn't need to, and for helping us troubleshoot problems with our protein purifications early in the project.

We would like to extend special thanks to the newest member of the lab, Alka Kumari, for coming in and making the changes necessary for future projects to succeed.

We would additionally like to thank the other members of the Dempski Lab for helping us when we needed it and for making the lab a comfortable working environment. Thanks Ryan Richards and Olga Gaiko.

We would like to extend our appreciation to the members of the Arguello Lab for allowing us to share their rotor, centrifuge, incubators, and generally for putting up with us. Without their generosity and tolerance, this project would not have been possible.

TABLE OF CONTENTS

TABLE OF FIGURES

TABLE OF TABLES

1. INTRODUCTION

Zinc is a physiologically crucial metal involved in many diverse cellular processes. In comparison to other transition metals that are required for biological function, zinc is the second most abundant (John et. al. 2010). Diseases and deficiencies associated with zinc uptake and homeostasis affect millions of people world-wide, providing the impetus for the study of zinc transporting proteins and their mechanisms of action (Ackland 2006). Among zinc transporter proteins, human ZIP4 was the focus of research for this project due to its involvement in the rare genetic disorder *acrodermatitis enteropathica* and pancreatic cancer (Zhang 2010). The intracellular region between transmembrane domains III and IV was expressed in *E. coli* and purified using affinity column chromatography. Zn^{2+} binding affinity assays were carried out using fluorescence spectroscopy and isothermal titration calorimetry. A conformational change upon Zn^{2+} binding was measured using circular dichroism. This project developed the protocols for expression and purification of the ZIP4 intracellular region to be analyzed with the methods above.

The human body utilizes zinc for a number of important purposes: for structure, catalysis, nutrition, and the active support of cellular metabolism among others (Vallee and Auld 1990). Zinc finger proteins utilize zinc as a structural component and many bind DNA, acting as transcription factors involved in gene expression and often in regulation (Creighton 1993). Alcohol dehydrogenase has zinc in its active site which helps to coordinate alcohol for catalysis (Vallee and Auld 1990). Zinc deficiency can cause immune response problems, cell growth issues, and even neuronal buildup of β-amyloid plaques in Alzheimer's (John et. al. 2010, Sensi et. al. 2009).

Once zinc is ingested with food and drink, it is absorbed from the gut and from the blood through zinc transport proteins which move the zinc into cells where it can be used. The family involved in zinc influx is referred to as the ZIP family for Zrt & Irt like protein (Eide 2004). The gene family which

encodes for the ZIP family of zinc transporters is classified as SLC39 (solute-linked carrier 39) (Lichten 2009). The counterpart to the ZIP family of zinc transporters involved in zinc influx is the ZnT family (SLC30), the members of which are involved in zinc efflux. The zinc transporters are expressed commonly across all phyla and can be found in most tissue types due to the physiological importance of zinc for cellular function. The proteins are membrane bound because they transport zinc and other metal ions which generally can't permeate through plasma- and vesicular-membranes. The superficial characteristics common to members of the ZIP family are eight transmembrane passes, N and C terminal ends on the same extracellular or extravesicular face, and an intracellular loop region of varying length between transmembrane domains III and IV.

The specific member of the ZIP family which was the focus of this project was ZIP4, the proposed structure of which is found in Figure 1. ZIP4 is an integral membrane protein that has a long (about 50% of the protein) N-terminal domain on the extracellular face, and an intracellular loop of seventy six amino acid residues between transmembrane domains III and IV (Amino acids 423- 499). ZIP4 is encoded by the SLC39A4 gene located at the human chromosome region 8q24.3 (Andrews 2008). The more abundant isoform encodes for a 647 amino acid protein (Schmitt 2009). Extracellular, solvent accessible histidine residues have been shown to be important for zinc cationic coordination and may be necessary for proper intracellular transport (Antala 2012). However, the exact method of transport is unknown.. The M3M4 intracellular region has a histidine rich motif (438- HSSHSHGGHSH-448) that may act as a sensor for high levels of intracellular zinc, activating an ubiquitination event upon zinc binding which could result in the degradation of the protein to prevent further zinc influx (Mao 2007).

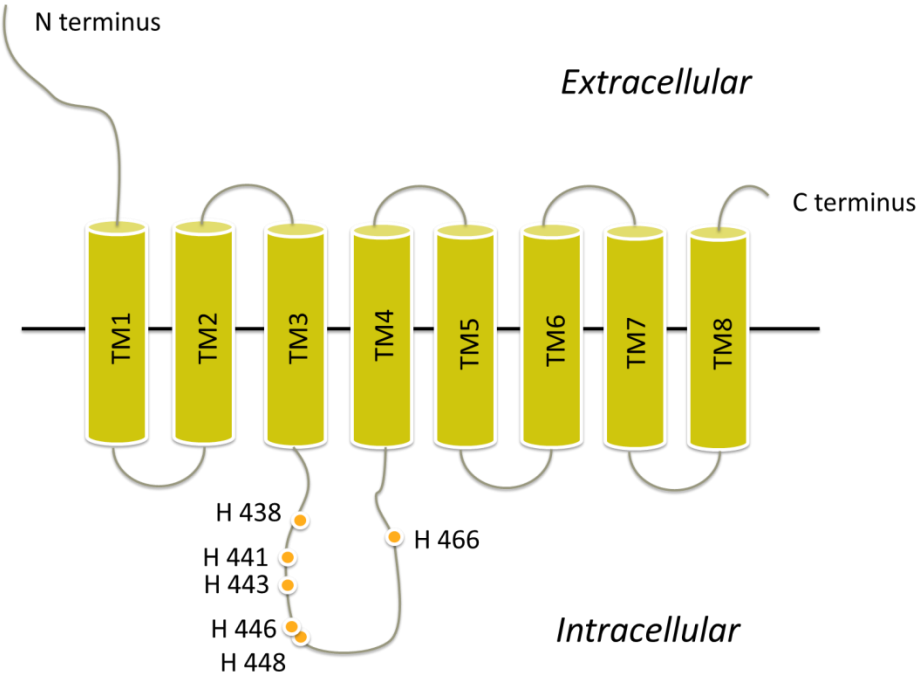

Figure 1: Proposed hZIP4 structure. Histidine residues on the M3M4 intracellular loop are highlighted in orange and numbered.

Zinc deficiency is a problem afflicting millions of people worldwide and can cause multiple symptoms, including immune system dysfunction, skin lesions, neurological disorders, and growth retardation. Mutations in the ZIP4 gene result in the ZIP4 protein being retained in the endoplasmic reticulum or having reduced functionality, leading to the disease acrodermatitis enteropathica (AE) (Andrews 2008). AE is an autosomal recessive disease believed to be caused by an inability to absorb sufficient zinc in the intestine (Andrews 2008).

ZIP4 overexpression has also been linked to pancreatic cancer. Zinc transporters are known to play an important role in regulating intracellular zinc concentration, which ultimately can affect cancer cell proliferation and metastasis by supporting enzyme activity (Donahue and Hines 2010). Mouse models with pancreatic cancer and forced overexpression of the ZIP4 gene were shown to have significantly larger tumors when compared to mice with normal levels of expression (Li et. al. 2007). Recent studies have also shown that the overexpression of ZIP4 may activate a novel pathway in which cyclin D1 expression is increased, resulting in increased cancer cell proliferation. ZIP4 and other factors

involved in the pathway may become therapeutic targets in the treatment of pancreatic cancer (Zhang et. al. 2010).

Previous research conducted in the Dempski lab sought to determine whether or not zinc would bind to the wild type M3M4 domain and what structural changes might occur within the domain in the presence and absence of Zn^{2+}. The proposed Zn^{2+} binding site was a histidine-rich motif, due to the high zinc binding affinity of histidine. Using atomic absorbance spectroscopy and fluorescence spectroscopy, it was determined that Zn^{2+}binds to the M3M4 domain with an affinity of 280 ± 50 nm and that the domain has two independent binding sites (Nguyen 2011). It was also shown, using native gel electrophoresis and circular dichroism, that the M3M4 domain undergoes a conformational change in the presence of Zn^{2+}. During the course of research, six single point mutant constructs were also generated corresponding to the six histidine residues implicated in zinc binding (Nguyen 2011).

The initial goal of this project was to further define the proposed zinc binding region for the ZIP4 zinc transporter by expressing and purifying the M3M4 wild type and mutant proteins and subjecting them to a variety of zinc binding assays. Our hypothesis was that mutations in the first five histidine residues in the M3M4 sequence would have a significant effect on the protein's zinc binding affinity, while the mutation in the sixth histidine residue would have a lesser effect. However, due to complications in the protein purification process, our project was refocused on the optimization of the protein purification protocol for the wild type protein. The wild type M3M4 protein was also subjected to zinc binding assays, including fluorescent spectroscopy, isothermal titration calorimetry, and circular dichroism. The results of these assays confirmed previous data.

2. MATERIALS AND METHODS

2.1 CELL CULTURE

20 µl of *E. coli* strain BL-21 (star) DE3 pLysS 1240 (Invitrogen) cells were transformed with a sample of DNA at 100 µg/ml using electroporation. A Cell-porator GIBCO BRL Electroporation Apparatus (Life-Technologies™) was used to allow the uptake of a pPR-IBA1 vector with M3M4 intracellular region gene inserted. Figure 2 shows the plasmid vector with inserted genes and labeled restriction sites. The transformed cells are incubated for one hour in 1 mL of SOC media on a shaker at 37°C. After incubation, the cells are plated on LB agar plates containing ampicillin (100 mg/mL), spectinomycin (50 mg/mL), and chloramphenicol (34 mg/mL) and left in an incubator overnight at 37°C.

The following day, a 50 mL startup culture was created by adding 50 µl each of ampicillin (100 mg/mL), spectinomycin (50 mg/mL), and chloramphenicol (34 mg/mL) to 50 mL of LB media in a 250mL glass Erlenmeyer flask. A single colony from one of the plates was transferred to the flask. The 50 mL startup culture was placed on a shaker at 37°C and incubated for 14 to 16 hours.

Two-1 L auto-induction cultures were made by adding 1 mL trace metal stock solution (50 mM $FeCl_3$, 20 mM $CaCl_2$, 10 mM $MnCl_2$, 10 mM $ZnSO_4$, 2 mM $CoCl_2$, 2 mM $NiCl_2$, 60 mM HCl), 1 mL magnesium sulfate, 1 mL ampicillin (100 mg/mL), 1 mL spectinomycin (50 mg/mL), 1 mL chloramphenicol (34 mg/mL), 25 mL glucose stock (2.5% glucose in ddH_2O), 25 mL glycerol stock (25% glycerol in ddH_2O), 25 mL salt stock (1 M Na_2HPO_4, 1 M KH_2PO_4, 0.5 M $(NH_4)_2SO_4$) in ddH_2O), and 2 g lactose to each 1 L of LB. Lastly, 20 mL of the startup culture was added to each flask and then placed on a shaker set to a speed of 180 rpm at 37°C for 6 hours. After 6 hours, the incubator settings were changed to 25°C and 200rpm and incubated for another 19-20 hours.

2.2 PROTEIN PURIFICATION

1 L of the auto-induction culture of transformed BL-21 *E. coli* was spun down in weigh-balanced plastic centrifuge bottles using a Sorvall RC-5B Refrigerated Superspeed Centrifuge and a fixed angle GSA rotor (diameter- 31cm, angle- 28^{o}) at 5,000 rpm for 15 minutes at 4 ℃. The supernatant was poured off and the other half of the liquid culture was poured into the same bottles, weigh-balanced, and spun again at 5,000 rpm for 15 minutes at 4 ℃. The supernatant was decanted and the bottles containing the pellets were then placed on ice for the duration of the resuspension step. The pellets were then resuspended in 50 mL of wash buffer (100 mM Tris-Cl pH 8.0, 150 mM NaCl) containing 1 mM Phenylmethylsulfonyl Fluoride (PMSF, MW 174.2) using a vortex machine. The contents of each bottle were combined and fully resuspended in two plastic 50 mL conical tubes.

The resuspended pellets were kept on ice for the duration of a sonication step. The resuspended cells were lysed using a Fisher Scientific Sonic Dismembrator Model 100, set to a power level of seven, for six periods of thirty second bursts followed by thirty seconds rest on ice. The fully sonicated cell lysate was then transferred in 1 mL aliquots to 2 mL plastic Eppendorf tubes and spun in a tabletop centrifuge at 15,000 rcf for 15 minutes at 4℃. The supernatant containing the soluble protein was transferred into a plastic 50 mL conical tube labeled cell lysate. 1 mL of the cell lysate was set aside and kept at 4 ℃ to be analyzed later using SDS-PAGE. 2 mL of Strep-Tactin® Superflow® resin (IBA) was packed into a 20 mL plastic column (Bio-Rad) with a flow control nozzle. The resin was flushed with regeneration buffer (100 mM Tris-Cl pH 8.0, 150 mM NaCL, 1 mM (4-hydroxy phenolazo) benzoic acid, MW 242.23) with 1 mM PMSF. The column was washed with wash buffer until the resin became clear (regeneration leaves the resin with an orange/yellow color). The lysate was then incubated with the washed resin at 4℃ on a shaker for an hour.

The cell lysate/resin mixture was added to the plastic column and the resin allowed to settle for five minutes before opening the stopcock and collecting flow-through at a rate of approximately 12

drops per minute. 1 mL of the flow-through was set aside and kept at 4 ℃ to be analyzed later using SDS-PAGE. 50 mL of wash buffer containing 1 mM PMSF was pipetted into the column without disturbing it, and the wash was collected. 1 mL of the wash was set aside and kept at 4 ℃ to be analyzed later using SDS-PAGE. 8 mL of elution buffer (100 mM Tris-Cl pH 8.0, 150 mM NaCl, 2.5 mM desthiobiotin, MW 214.76) with 1 mM PMSF was added to elute the protein which remained bound to the column and 1 mL elution fractions were collected. The column was then regenerated until the resin returned to a bright orange color. Each elution was checked for protein presence using a Bradford Assay (Bradford 1976) and absorbance was measured at 280 nm using a NanoDrop 2000c Spectrophotometer (Thermo Scientific) in order to calculate the protein concentration.

2.3 SDS-POLYACRYLAMIDE GEL ELECTROPHORESIS

20 µl of 6x Laemmlli sample buffer (100 mM Tris, pH 6.8, 2% SDS, 5% β-mercaptoethanol, 15% glycerol, and 0.012% (w/v) bromophenol blue) was added to each protein sample (30 µl of cell lysate, flow through, and wash, 100 µl of each elution). The samples were incubated at 90°C for three minutes and then loaded into the wells on two 15% SDS-polyacrylamide gels. The gels were run at 40 mA and stopped once the dye reached the bottom (approximately 100 minutes).

Before staining the gel, the stacking gel was removed from the separating gel and discarded. The separating gel was then placed in 50 mL of Coomassie staining solution (0.025% Coomassie blue G-250, 10% acetic acid, 90% ddH_2O) to stain non-specifically for protein. The gel was stained at room temperature on a shaker overnight. The staining solution was discarded and 50 mL of destaining solution (7% glacial acetic acid, 5% methanol, and 88% ddH_2O) was added on top of the gel. The gel was destained for approximately four to five hours, until the gel became colorless but the bands remained blue stained.

The second gel was used for Western blot analysis to show the presence of the hZIP M3M4 intracellular region. The stacking gel was discarded and the separating gel was placed directly on a PVDF

membrane pressed between cotton absorbent pads and the apparatus was then placed in Western transfer buffer (25 mM Tris, 20 mM Glycine, and 20% (w/v) methanol) and run on a Western transfer device at 100 V for one hour. The membrane with transferred protein was then blocked either for 1 hour at 25℃ or overnight at 4℃ with TBS and 1% tween with 2 mL 2 mg/mL BSA. The membrane was washed 3 times with TBS and 1% tween then incubated for 1 hour at 25℃ with a monoclonal Strep-Tactin antibody. The membrane was washed 3 times with TBS and 1% tween and then developed using an AP Conjugate Substrate Kit (Bio-Rad).

2.4 BUFFER EXCHANGE AND DYNAMIC LIGHT SCATTERING

Following column purification and a check for protein presence using a Bradford assay, the elution fractions testing positive for protein were then pooled together and distributed into four equal volumes which were dialyzed overnight in four different buffer conditions: 1) 20 mM Trizma, pH 7.8 with 150 mM NaCL 2) 20 mM Trizma, pH 7.8 with 150 mM NaCL and 5% Glycerol 3) 20 mM Trizma, pH 7.8 with 150 mM NaCl and 10% Glycerol 4) 20 mM Trizma, pH 7.8 with 150 mM NaCL and 20% Glycerol. The dialyzed protein was then transferred to 1.5 mL Eppendorf tubes for further testing. After buffer exchange via dialysis, the protein was then checked for aggregation using Dynamic Light Scattering (DLS).

2.5 ISOTHERMAL TITRATION CALORIMETRY

A 0.16 mM zinc chloride solution was made using the same Trizma buffer used during the buffer exchange. The M3M4wt protein and the zinc chloride were degassed prior to each titration. The following protocol was based on the protocol found in the instrument manual (TA Instruments 2010). The reference cell was filled with deionized water and 6 µM M3M4 was placed in the reaction cell. The instrument was equilibrated for 2000 seconds to 10 °C. Twenty consecutive injections of 2.5 µl of zinc chloride were made at 300 second intervals with a stirring rate of 250 rpm.

2.6 CIRCULAR DISCHROISM

Due to the fact that Zn^{2+} will easily precipitate with phosphate, a pH 7.8 10 mM Trizma and 30 mM NaCl buffer was used in dialysis with sample M3M4 protein rather than phosphate buffer which is commonly used in CD experiments. The samples were run through a Chelex-100 column to remove trace zinc and other divalent cations which could skew the zinc binding study. 300 µL mixtures were made containing 6 nM purified M3M4 protein with 0.015 nM, 0.15 nM, 1.5 nM, 3 nM, 6 nM, and 9 nM zinc chloride ($ZnCl_2$). The protein and zinc were incubated 5 minutes prior to scanning to ensure appropriate chance for binding and complex formation. CD scans were done using a Jasco J715 spectropolarimeter using a Peltier thermostated sample holder for thermal melts. Scans were done in triplicate according to the conditions listed in Table 1. Measurements made in millidegrees were converted to elipticity (θ- mdeg cm^2/dmole) by way of the following equation:

$$\theta = \frac{CD\ signal\ in\ millidegrees}{(cuvette\ path\ length\ in\ mm) * (protein\ concentration) * (number\ of\ residues)}$$

CD Run Parameter	Setting
Sensitivity standard	100 mdeg
Start	270 nm
End	190 nm
Data pitch	0.5 nm
Scanning mode	Continuous
Scanning speed	20 nm/min
Response	8 seconds
Band Width	2.0 nm
Accumulation	3
Temperature	4°C
Cell 1 mm for	200 µl

Table 1: CD parameters and settings for control and zinc binding runs.

3. RESULTS

3.1 PROTEIN PURIFICATION

Initially, the BL-21 *E. coli* cells were grown in liquid culture at 37°C and induced at 37°C overnight. However, the amount of purified protein was lower than expected. The manufacturer of the Step-tag recommends that the cells be grown at a lower temperature in order to slow growth and to increase the solubilization of the protein. An experiment was devised in order to select the most optimal auto-induction temperature and incubation time with the highest resulting protein expression (see Table 2). The expression of the protein was approximated by the intensity of the appropriate bands on a Western blot. The auto-induction temperature of 25°C and incubation time of 8 hours yielded the highest concentration of protein and more consistent results.

Other changes were made to protein purification protocol to prevent protein degradation and promote protein to zinc binding conditions. 1 mM PMSF, a protease inhibitor, was added to each of the protein purification buffers: Buffer W, Buffer R, and Buffer E. The addition of PMSF helped to prevent proteases from degrading the protein and rendering it less functional. The original buffer recipes called for EDTA (ethylenediamminetetraacetate), which chelates divalent cations which may be present in the cell lysate. EDTA was removed from the recipe in order to prevent interference with zinc binding during the zinc binding assays. The resin washing step of the protein purification protocol, after the cell lysate incubation, was also increased from 10 mL to 50 mL of Buffer W to reduce the amount of nonspecific protein binding to the resin.

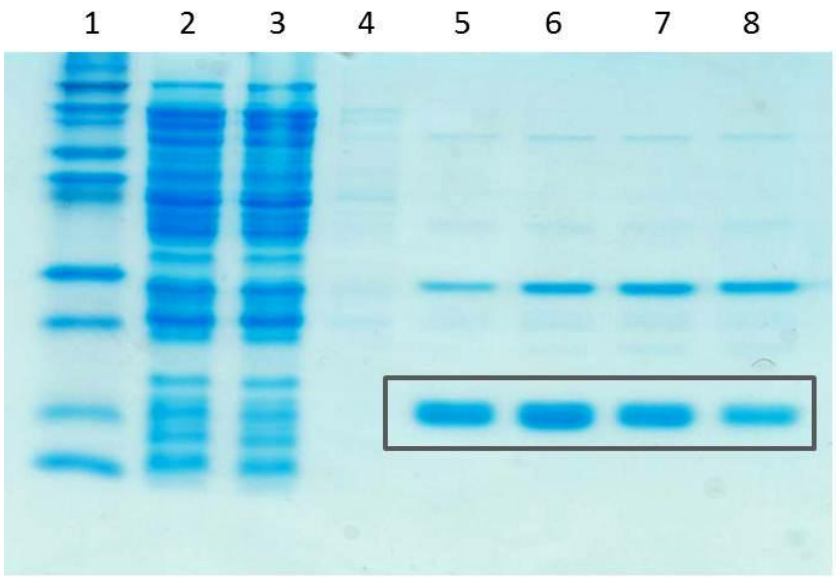

Figure 2: Coomassie stained 12% polyacrylamide gel of M3M4wt protein. 10 µl of protein ladder, cell lysate, flow through, and wash, and 20 µl of elution loaded. (1) Novex® Sharp Standard Protein ladder (260-3.5 kDa) (2) Cell lysate (3) Flow through (4) Wash (5-8) Elution fractions. M3M4wt bands highlighted in grey box. M3M4wt runs at ~12 kDa.

Figure 2 shows a polyacrylamide gel stained with coomassie-blue-G250 which was taken during pre-optimization of the protein purification procedure. The boxed bands show the M3M4 protein, which comes out on the gel at about 12 kDa. While this pre-optimization gel still shows nonspecific protein bands, gels from after the protein protocol was optimized showed only traces of nonspecific protein.

3.2 DYNAMIC LIGHT SCATTERING

Each dialysis condition was tested using DLS for protein aggregation to determine which (if any) of the buffer exchange conditions would have an effect on the stability of the protein in solution. Figure 3a shows the DLS scan for the purified hZIP4 M3M4 intracellular region before dialysis presented as a plot of % volume distribution against average spherical diameter in nanometers. A peak just before 10 nm shows a monodisperse population of protein at a low average hydrodynamic diameter. Figure 3b presents the results obtained for DLS scans of the same protein sample after dialysis in four different

conditions for buffer replacement. The red line signifying the measurement for buffer without glycerol yields a different plot than the protein before dialysis which could be due to the amount of time since purification or due to the solubility of the protein in the different buffer system. The plot shows a percentage of the protein has an average diameter above 1000 nm signifying aggregation has begun. The 5% glycerol sample (presented as a green line) was more polydisperse and had a higher volume % closer to 10 nm diameter and a less concentrated peak above 1000 nm than the sample ran in buffer without glycerol. The other two samples containing 10 and 20% glycerol show a monodisperse population of protein with a very large volume % of the population above 1000 nm which suggests that glycerol above 5% in solution can cause significant aggregation.

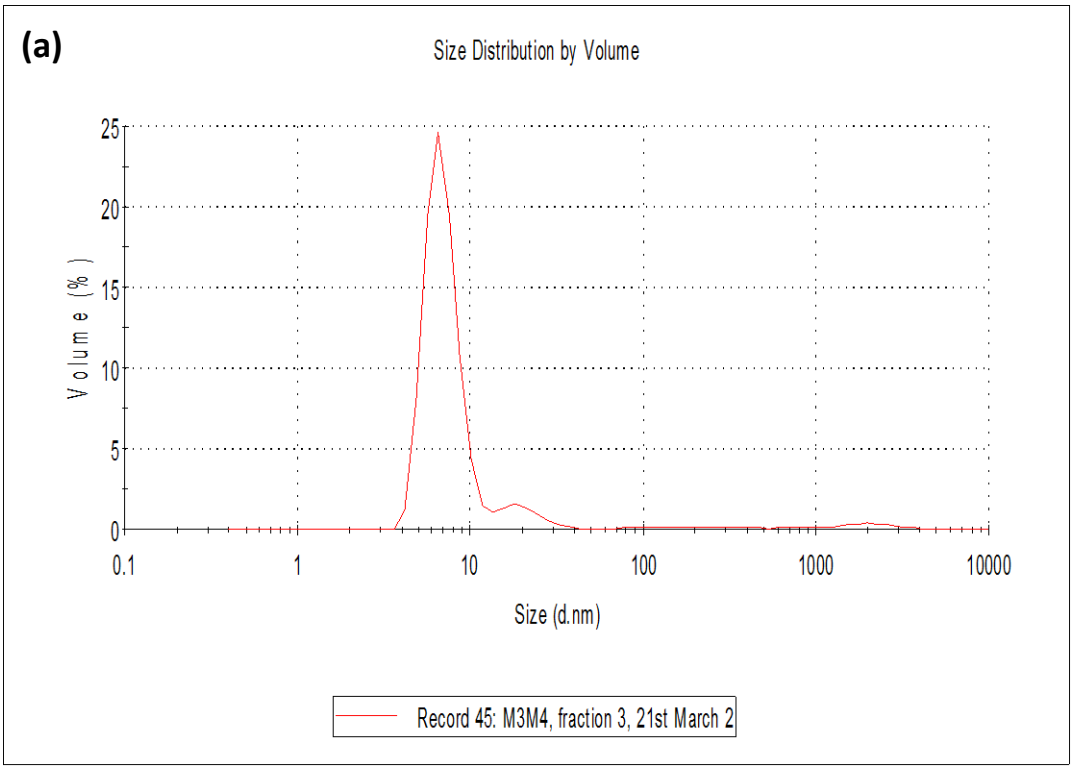

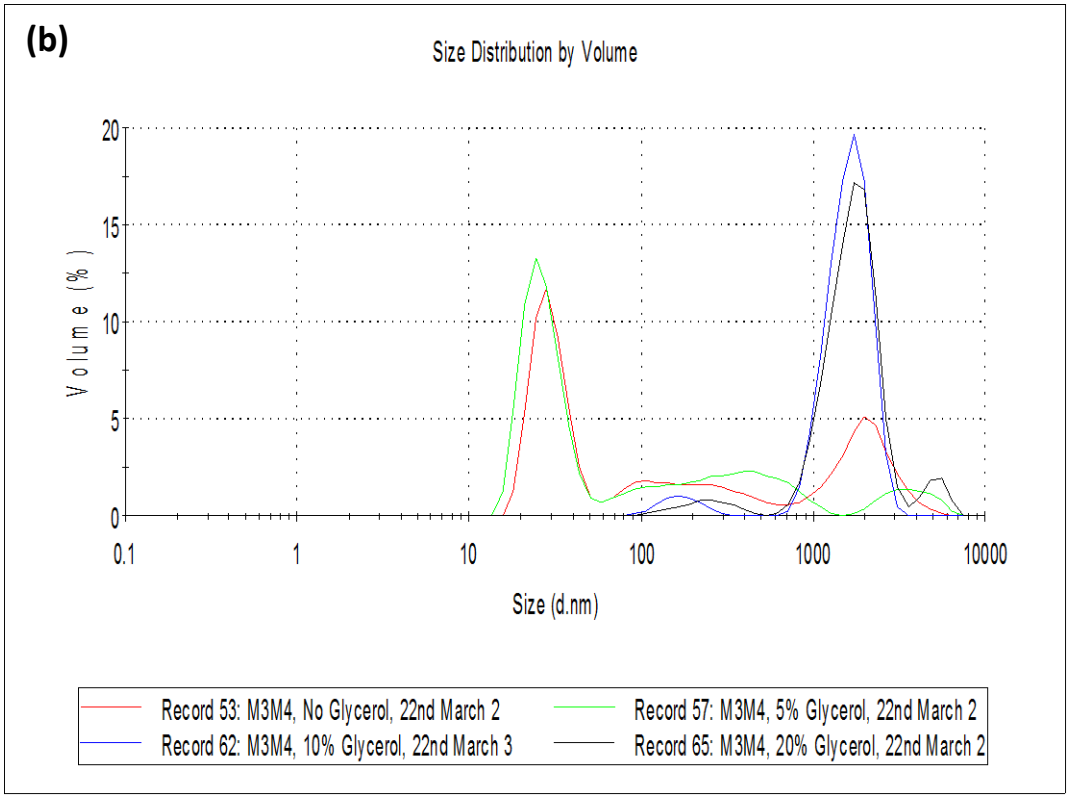

Figure 3: Dynamic Light Scattering of M3M4wt. (a) M3M4wt protein in elution buffer before buffer exchange (b) M3M4wt protein after dialysis in Trizma buffer (30 mM Trizma, 150 mM NaCl, pH 7.4) with 0%, 5%, 10%, and 20% glycerol. Data generated by Alka Kumari.

3.3 ISOTHERMAL TITRATION CALORIMETRY

The result of an ITC measurement for a single sample of 6 µM M3M4 protein in Trizma buffer without glycerol in a reaction mixture with 0.16 µM Zn^{2+} can be seen in Figure 4. Every injection point on the figure is signified by a peak which represents a rise in enthalpy in solution, a characteristic of zinc binding free protein. At early time points, more protein is free and able to bind zinc; therefore the first peak has the greatest energy increase upon zinc binding than each consecutive peak.

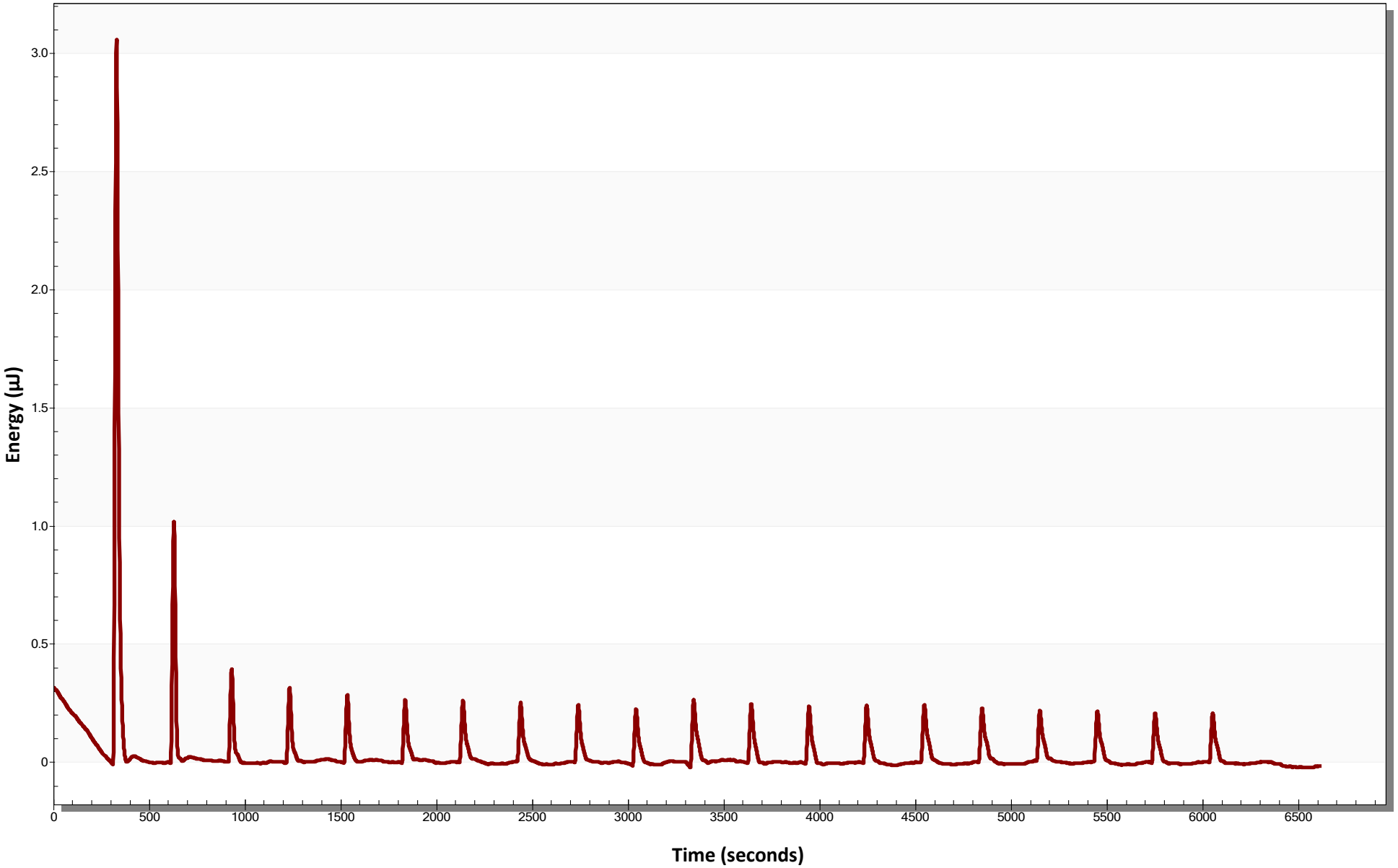

Figure 4: ITC curve for M3M4wt in Trizma buffer. 6 µM M3M4wt incubated with twenty injections of 2.5 µl increments of 0.16 mM Zn^{2+} at a stir rate of 250 rpm. Data generated by Alka Kumari.

3.4 CIRCULAR DICHROISM

The CD run for 6 nM purified M3M4 protein shows a local minimum ellipticity value of -4.5 mθ around a wavelength of 200nm and is the only defining characteristic found on the plot presented in Figure 5. A large change can be seen in the overall ellipticity measurements for the protein incubated with zinc compared to protein not incubated with zinc, however, varying the zinc concentration while also maintaining the concentration of purified M3M4 in the reaction mixture constant appeared to have little effect on the ellipticity. Zinc incubated samples resulted in a deep trough averaging at -15.6 mθ at a wavelength of 200 nm which is a three-fold increase over the protein alone.

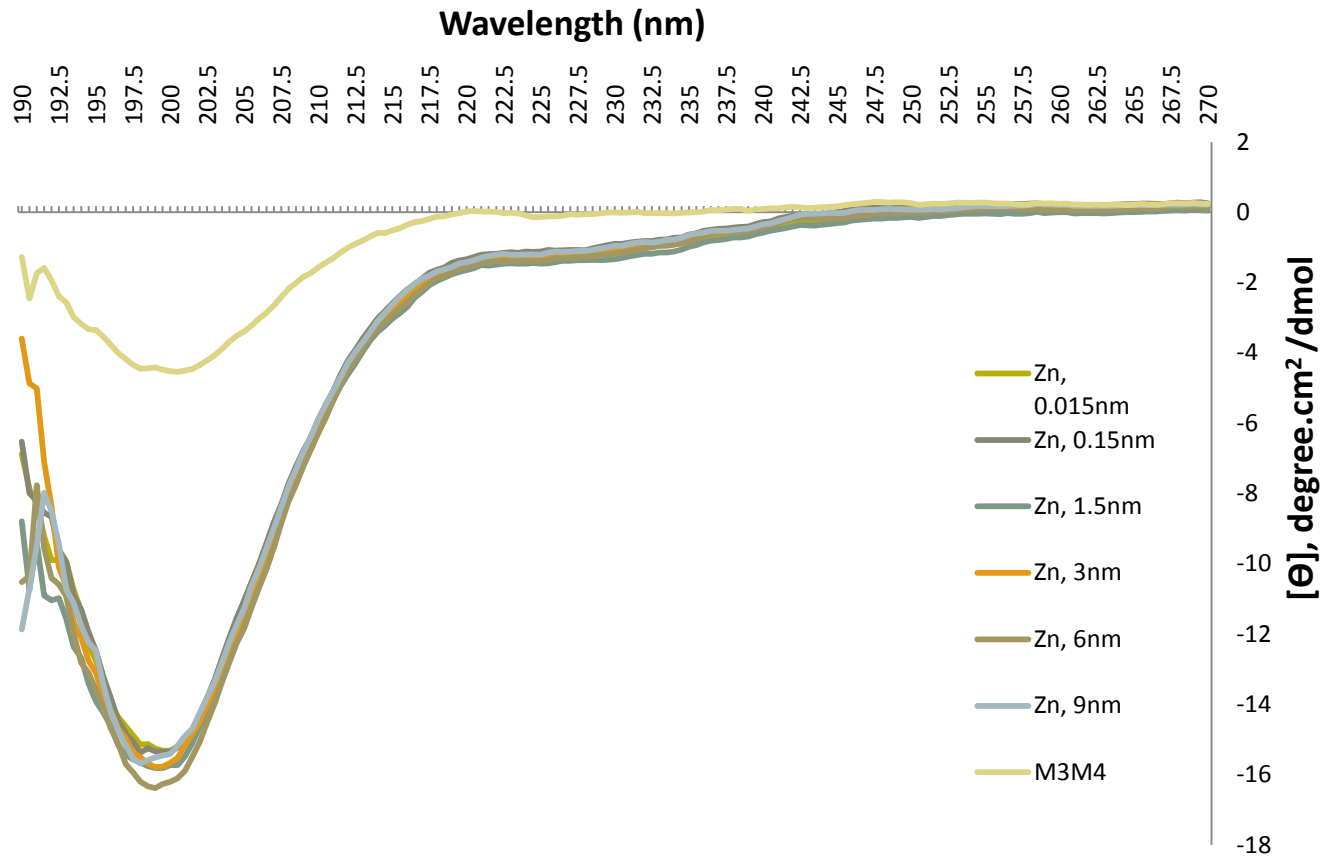

Figure 5: CD scan data. M3M4wt protein and M3M4 protein incubated with 0.015 nm, 0.15 nm, 1.5 nm, 3 nm, 6 nm, and 9 nm Zn^{2+}. Data generated by Alka Kumari.

The CD data was analyzed using the modified k2d algorithm, for wavelengths 190 to 240 nm, to predict the secondary structure of M3M4wt protein incubated with and without Zn^{2+} (Per Unneberg 2001). The percentage of alpha helices and beta pleated sheets decreased significantly upon incubation with zinc. The M3M4wt incubated with zinc shows a shift to a more random predicted structure likely caused by the presence and binding of zinc.

	M3M4wt (%)	M3M4wt with Zn^{2+} (%)
Alpha	18.2 ± 2.5	1.0 ± 4.1
Beta	27.6 ± 6.7	2.1 ± 8.2
Turn	14.9 ± 6.1	0.9 ± 3.6
Random	39.3 ± 1.4	96.0 ± 15.8

Table 2: Secondary structure estimation from CD data. Predictions were made using the CD data for 6 nm M3M4wt and an average of all CD data of M3M4wt incubated with Zn^{2+} for 190 to 240 nm.

5. DISCUSSION

Many changes were made to the protein expression and purification protocols that had previously been developed and used. Lengthening the incubation time of the 2 L liquid culture from 19 to 25 hours, combined with lowering the induction temperature to 25^{o}C after 6 hours, increased the protein yields. The 2 L liquid culture was also split into two 1 L liquid cultures and the run speed of the shaker/incubator was increased from 180 to 200 rpm in order to increase air flow to the cells and to allow for even mixing during growth phases. The addition of 1 mM PMSF, a protease inhibitor, to all buffers during purification ensured that a greater proportion of the purified protein was left intact and not degraded by proteases. Besides adding protease inhibitor to all buffers, a particular component of the buffers which may have contributed to non-typical behavior of the protein during zinc binding assays was EDTA. EDTA binds divalent cations (like Zn^{2+}) with high affinity and its presence in solution required that the samples be spun down and the elution buffer replaced with Tris or Trizma buffer in order to remove trace EDTA before zinc binding assays. A more effective way of dealing with the problem was leaving EDTA out of the purification buffers in the first place. In order to increase the purity of the collected protein fractions from the strep-tag affinity column, the column was washed with a greater volume of wash buffer to decrease the amounts of non-specific protein remaining in the purified samples. Due to the apparent aggregation of the protein at higher concentrations of glycerol measured by dynamic light scattering, the buffer exchange was best carried out with either 5% glycerol in Trizma buffer or in Trizma alone. Overall, these changes resulted in a decrease in nonspecific protein binding to the strep-tag column, an increase in targeted protein yield, and the setup of a reliable and consistent protein purification protocol.

After developing a sufficient method to generate high yields of the target protein, two zinc binding assays, isothermal titration calorimetry and circular dichroism, were performed. ITC measures the power (converted to enthalpy) required to maintain a constant temperature of a mixture in which

protein-protein interactions or protein-ligand interactions cause a change in enthalpy. The preliminary ITC data indicates that at low nanomolar concentrations of zinc, the M3M4 intracellular region of the hZIP4 protein binds zinc cations, however, further experiments must be performed to confirm whether zinc is binding and with what stoichiometry. Circular dichroism is a method that can be used to elucidate the secondary structure characteristics of a purified protein and to gauge specific protein conformations caused by interactions with ligands or with other proteins. For the M3M4 intracellular region of the hZIP4 protein, it appears that in the presence of Zn^{2+} there is a significant change in conformation as evidenced by the deep trough at 200 nm on the plot in Figure 5 which was a three-fold greater value than the M3M4 protein alone. This deep trough is thought to be result of the binding of the Zn^{2+} with the histidine residues found in this portion of ZIP4. This binding and corresponding conformational change was observed for Zn^{2+} at all nanomolar concentrations tested.

This major qualifying project has optimized the purification protocol for higher and purer yields of hZIP4 M3M4 intracellular region than were achieved in previous experiments. With the new protocol for expression and purification in place and optimized, it is now possible to do extended research with six single mutant M3M4 constructs (histidine to alanine) which have been prepared. It is also necessary for the zinc binding assays to be optimized and repeated for the confirmation of results. These experiments can help determine the specific histidine residues involved in zinc binding and data collected can be easily compared to experiments done with wild type M3M4 intracellular region.

REFERENCES

Ackland ML, Michalczyk A. 2006. Zinc deficiency and its inherited disorders –a review. Genes Nutr. 1:41-49.

Andrews G. 2008. Regulation and function of ZIP4, the acrodermatitis enteropathica gene. Biochem. Soc. Trans. 36:1242-1246.

Antala S, Dempski RE. 2012. The human ZIP4 transported has two distinct binding affinities and mediates transport of multiple transition metals. Biochem. 51:963-973.

Creighton TE. 1993. Proteins. In: Relationship Between Protein Conformation and Binding. New York: W. H. Freeman and Company. p 348.

Donahue T, Hines OJ. 2010. The ZIP4 pathway in pancreatic cancer. Canc. Biol. Thera. 9:243-245.

Eide DJ. 2004. The SLC39 family of metal ion transporters. Pflügers Archiv European Journal of Physiology. 5: 796-800.

Grimsley GR, Pace CN. 2003. Spectrophotmetric determination of protein concentration. In: Current Protocols in Protein Science. New York: John Wiley & Sons, Inc. p 33-44.

Haigh EA, Sawyer WH. 1978. Interpretation of double reciprocal plots used to determine the spectroscopic parameters of bound ligand for binding assays. Aust. J. Biol. Sci. 31: 1-5.

John E, Laskow TC, Buchser WJ, Pitt BR, Basse PH, Butterfield LH, Kalinski P, Lotze MT. 2010. Zinc in innate and adaptive tumor immunity. J. Trans. Med. 8:118.

Li M, Zhang Y, Liu Z, Bharadwaj U, Wang H, Wang X, Zhang S, Liuzzi JP, Chang S, Cousins RJ, Fisher WE, Brunicardi F, Logsdon CD, Chen C, Yao Q. 2007. Abberant expression of zinc transporter ZIP4 (SLC39A4) significantly contributes to human pancreatic cancer pathogenesis and progression. PNAS. 47:18636-18641.

Lichten LA, Cousins RJ. 2009. Mammalian zinc transporters: nutritional and physologic regulation. Annu. Rev. Nutr. 29:153-176.

Mao X, Byung-Eun K, Wang F, Eide DJ, Petris MJ. 2007. A Histidine-rich cluster mediates the ubiquitination and degradation of the human zinc transporter, hZIP4, and protects against zinc cytotoxicity. J. Biol. Chem. 282:6992-7000.

Nguyen T. 2011. Investigating the properties of the ZIP4 M3M4 domain in the presence and absence of Zn^{2+}. Masters Thesis. Worcester Polytechnic Institute.

Per Unneberg, Juan J. Merelo, Pablo Chacón, Federico Morán, *SOMCD: Method for evaluating protein secondary structure from UV circular dichroism spectra*, Proteins: Structure, Function, and Genetics, vol. 42, no. 4; pages 460-470; 2001; http://dx.doi.org/10.1002/1097-0134(20010301)42:4<460::AID-PROT50>3.0.CO;2-U

Schmitt S, Kury S, Giraud M, Dreno B, Kharfi M, Bezieau S. 2009. An update of mutations of the SLC39A4 gene in acrodermatitis enteropathica. Hum. Muta. 30:926-933.

Sensi SL, Paoletti P, Bush AI, Sekler I. 2009. Zinc in the physiology and pathology of the CNS. Nat. Rev. Neurosci. 10: 780-791.

TA Instruments. 2010. Nano Isothermal Titration Calorimeter: Getting Started Guide for Models 601000, 601001, 601002. p42.

Taylor KM, Nicholson RI. 2003. The LZT proteins; the LIV-1 subfamily of zinc transporters. Biochim. Biophys. Acta. 1611:16-30.

Truong-Tran AQ, Ho LH, Chai F, Zalewski PD. 2000. Cellular zinc fluxes and the regulation of apoptosis/gene-directed cell death. J. Nutr. 130:1459-1466.

Vallee BL, Auld DS. 1990. Zinc coordination, function, and structure of zinc enzymes and other proteins. Biochem. 24:5648-5658.

Zhang Y, Bharadwaj U, Logsdon CD, Chen C, Yao Q, Min L. 2010. ZIP4 regulates pancreatic cancer cell growth by activating IL-6/STAT3 pathway through zinc finger transcription factor CREB. Clin. Cancer Res. 16:1423-1430.